

An Artificial Frustrated System: Cold Atoms in Triangular Optical Lattice

Yao-Hua Chen, Wei Wu, Hong-Shuai Tao, and Wu-Ming Liu

Beijing National Laboratory for Condensed Matter Physics,
Institute of Physics, Chinese Academy of Sciences, Beijing 100190, China

(Dated: November 19, 2019)

We investigate the strongly correlated effect of cold atoms in triangular optical lattice by dynamical cluster approximation combining with the continuous time quantum Monte Carlo method proposed recently. It is found the double occupancy is suppressed as the atomic interaction increases. By calculating the density of states, we show how the system evolves from Fermi liquid with an obvious quasi-particle peak into Mott insulator with an opened gap for increasing interaction. The transition between Fermi liquid and pseudogap shows a reentrant behavior due to the Kondo effect. At low temperature, a Kondo peak appears before the splitting of the Fermi-liquid-like peak. The Fermi surface evolves from a circular ring with high amplitude into a flat elliptical ring with low amplitude for the increasing interaction. We give an experimental protocol to observe these phenomena by varying the lattice depth and the atomic interaction via Feshbach resonance in future experiments.

PACS numbers: 03.75.Ss, 03.75.Hh, 71.10.Fd

Introduction. — Quantum phase transition in strongly correlated system is an important research area in condensed matter physics, presenting some of the most challenging problems. In a real material, the experimental parameter is hard to be varied to observe the strongly correlated effect, which is complicated by impurities and multiple bands. However, a new developing technology called optical lattices presents a highly controllable and clean system for studying strongly correlated system, in which the relevant parameter can be adjusted independently [1–7]. Optical lattices with different geometrical property can be set up by adjusting the propagation directions of laser beams, such as triangular and honeycomb optical lattice [8–12]. The interaction between the trapped atoms is tunable through the Feshbach resonance, such as ^{87}Rb and ^{40}K . In recent years, a series of experiments have been carried out to investigate the quantum phase transition of cold atoms in optical lattice [13–17]. Comparing with a real material, the optical lattice is controllable and clearness.

There are many analytical and numerical methods to investigate the strongly correlated system, especially the frustrated system [18–27]. The dynamical mean-field theory (DMFT) [28] has been proved to be a useful tool. The self-energy is given as a local quantity in DMFT, which has been proved to be exact in the infinity dimensional limit [29, 30]. This method is a good approximation even in three dimensional situation [31]. However, in lower dimensional situation or the frustrated systems, the nonlocal correlations can not be simply ignored, DMFT would not work efficiently. So, many methods have been improved to incorporate nonlocal correlations in the framework of DMFT, such as dynamical cluster approximation (DCA) [32–34]. Different with the DMFT, the lattice problem is mapped into a self-consistently embedded finite-sized cluster in DCA. The irreducible quantities of the embedded cluster is used as an approximation for the

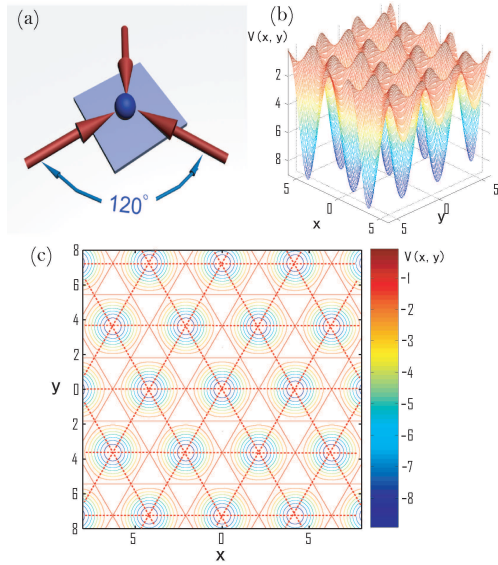


FIG. 1: (Color online) (a) Sketch of experimental setup to form triangular optical lattice. Each arrow depicts a laser beam, the sphere in the center of the figure depicts the fermionic quantum gas, such as ^{40}K . (b) Landscape of potential $V(x, y)$ in the x - y plane. (c) The contour lines of triangular optical lattice. The dark blue circles indicate the minimum lattice potential. The dash red lines show the geometry of this triangular optical lattice by connecting the minimum lattice potential.

corresponding lattice quantities. DCA has been used to investigate the geometrical frustrated system [35, 36].

In present Letter, we propose an artificial frustrated system – cold atoms in triangular optical lattice to observe the strongly correlated effect in condensed matter physics. We improve the numerical method – DCA combining with the continuous time quantum Monte Carlo method (CTQMC) [37] to investigate this geometrical

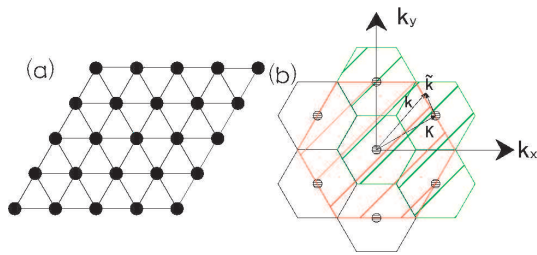


FIG. 2: (Color online)(a) Sketch of triangular lattice. (b) An example of coarse graining procedure in the first Brillouin Zone when $N_c = 4$. The red part shows the first Brillouin Zone in reciprocal space. The green part shows the region divided into 4 cells for DCA calculation. The \mathbf{K} is the cluster momentum used to represent the coarse graining cell, the \mathbf{k} is the momentum inside a cell, and the \mathbf{k} is the momentum in the first Brillouin Zone.

frustrated system. CTQMC, used as the impurity solver, is an exact numerical method proposed recently. By calculating the density of states and the spectral function, we find the system undergoes a second order phase transition from Fermi liquid with a quasi-particle peak to Mott insulator with an opened gap. The phase diagram shows a reentrant behavior of the transition between Fermi liquid and pseudogap due to the Kondo effect at low temperature. These phenomena can be observed in the triangular optical lattice by varying the lattice depth and the interaction strength via the Feshbach resonance. The advantage of this artificial frustrated system is highly controllable and cleanliness. And the numerical method acts as a powerful tool for investigating the strongly correlated effect in condensed matter physics, such as the spin liquid, the high-temperature superconductor and the colossal magnetoresistance.

Artificial Frustrated System. — In contrast with real materials, the fermionic atoms, such as ^{40}K , trapped in an optical lattice provide an artificial system to investigate the strongly correlated effect. The experiment can be performed with ^{40}K atoms prepared by mixing two magnetic sublevels of the $F = 9/2$ hyperfine manifold, such as the $| -9/2 \rangle$ and the $| -5/2 \rangle$ states [15]. As an artificial frustrated system, the triangular optical lattice can be set up by three laser beams, such as the Yb fiber laser at wavelength $\lambda = 1064$ nm, with a $2\pi/3$ angle between each other, as illustrated in Fig. 1(a). The potential of optical lattice [8] is given by

$$V(x, y) = V_0 \left(3 + 4 \cos\left(\frac{k_x x}{2}\right) \cos\left(\frac{\sqrt{3}k_y y}{2}\right) + 2 \cos(\sqrt{3}k_y y) \right), \quad (1)$$

where V_0 is the barrier height of standing wave formed by laser beams in the x-y plane, k_x and k_y are the two components of wave vector $k = 2\pi/\lambda$ along the x and y directions. In experiments, V_0 is always given in units of recoil energy $E_r = \hbar^2 k^2 / 2m$ [6]. The landscape of potential of triangular optical lattice in the x-y plane is

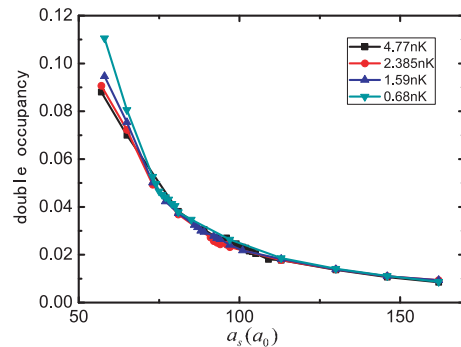


FIG. 3: (Color online) The double occupancy D_{occ} as a function of the interaction U which is indicated by the scattering length a_s for different temperature.

shown in Fig. 1(b), where the dark blue parts in the figure indicate the minimum lattice potential. Fig. 1(c) shows the contour lines of the triangular optical lattice. By connecting the center of the circular which indicates the minimum lattice potential, we may get the geometry of this triangular optical lattice, as shown by the red dash lines.

The Hamiltonian of the interacting fermionic atoms trapped in this artificial frustrated system is written as

$$H = -t \sum_{\langle ij \rangle \sigma} c_{i\sigma}^+ c_{j\sigma} + U \sum_i n_{i\uparrow} n_{i\downarrow}, \quad (2)$$

where $c_{i\sigma}^+$ and $c_{i\sigma}$ denote the creation and the annihilation operator of the fermionic atom on lattice site i respectively, $n_{i\sigma} = c_{i\sigma}^+ c_{i\sigma}$ represents the density operator of fermionic atom. And $t = (4/\sqrt{\pi})E_r(V_0/E_e)^{3/4} \exp(-2(V_0/E_r)^{1/2})$ is the kinetic energy, which can be adjusted by the lattice depth V_0 . $U = \sqrt{8/\pi} k a_s E_r (V_0/E_r)^{3/4}$ is the on-site interaction determined by the s-wave scattering length a_s , which can be adjusted by Feshbach resonance [7].

Numerical Method: DCA+CTQMC. — We improve the dynamical cluster approximation (DCA) to combine with the continuous time Quantum Monte Carlo method (CTQMC) to investigate the strongly correlated effect of cold atoms in the frustrated system shown in Fig. 2(a), which can be realized by Hubbard model (2).

In DCA, the reciprocal space of the lattice containing N points is divided into finite cells [33, 34]. The coarse-graining Green's function \bar{G} is achieved by averaging Green's function G within each cell. The lattice problem is mapped into a self-consistently embedded finite-sized cluster. The coarse graining procedure of the DCA is illustrated as follows: the Brillouin zone is divided into N_c cells, each cell is represented by a cluster momentum \vec{K} . In Fig. 2(b), we provide an example of this coarse graining procedure in $N_c = 4$ situation. In our treatment, the coarse-grained Green's function $\bar{G}(\vec{K}, i\omega_n) = \frac{N_c}{N} \sum_{\vec{k}} G(\vec{K} + \vec{k}, i\omega_n)$, where summation

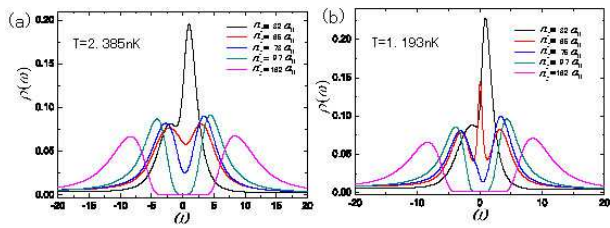


FIG. 4: (Color online) The density of states (DOS) as a function of frequency ω for different interaction. (a) At $T = 2.385nK$, a Fermi-liquid-like peak splits into two part and a pseudogap appears when the interaction increases. A gap is opened when the interaction is stronger than the critical interaction $a_s^c = 94a_0$. (b) At $T = 1.193nK$, a Kondo resonance peak is found before the pseudogap appears.

over $\tilde{\mathbf{k}}$ is taken within the coarse-graining cell, the ω_n is the Matsubara frequency.

Similar with DMFT, after mapping the Hubbard model to an Anderson impurity problem, we introduce an impurity solver, such as quantum Monte Carlo (QMC), fluctuation exchange approximate (FLEX), and the non-crossing approximation (NCA), to deal with the cluster problem. In our calculation, we employ the CTQMC [37] which does not need to introduce any auxiliary-field variables as our impurity solver. Comparing with the traditional QMC method, the CTQMC is much more exact, because it does not use the Trotter decomposition.

The self-consist loop can be taken as follows: 1) The DCA iteration loop can be started by setting the initial self-energy $\Sigma_c(\vec{\mathbf{K}}, i\omega_n)$ which can be guessed or be get from a perturbation theory. 2) We could get the $\bar{G}(\vec{\mathbf{K}}, i\omega_n) = \frac{N_c}{N} \sum_{\tilde{\mathbf{k}}} 1/(i\omega_n - \varepsilon_{\vec{\mathbf{K}}+\tilde{\mathbf{k}}} - \bar{\Sigma}_\sigma(\vec{\mathbf{K}}, i\omega_n))$. 3) The host Green's function $\bar{G}(\vec{\mathbf{K}}, i\omega_n)$ is computed by $\bar{G}(\vec{\mathbf{K}}, i\omega_n)^{-1} = \bar{G}(\vec{\mathbf{K}}, i\omega_n)^{-1} + \Sigma_c(\vec{\mathbf{K}}, i\omega_n)$. 4) The $\bar{G}(\vec{\mathbf{K}}, i\omega_n)$ is transformed from momentum-frequency variable to space-time variable $\bar{G}(\vec{\mathbf{X}}_i - \vec{\mathbf{X}}_j, \tau_i - \tau_j)$ used as the input to the CTQMC simulation. 5) The CTQMC step is the most time consuming part of the iteration loop. In our CTQMC step, we use 10^7 CTQMC sweeps. After the simulation, we get $\bar{G}(\vec{\mathbf{X}}_i - \vec{\mathbf{X}}_j, \tau_i - \tau_j)$. 6) $\bar{G}(\vec{\mathbf{X}}_i - \vec{\mathbf{X}}_j, \tau_i - \tau_j)$ is transformed from space-time variable to momentum-frequency variable $\bar{G}(\vec{\mathbf{K}}, i\omega_n)$ by Fourier transform. 7) We get the new self-energy by $\Sigma_c(\vec{\mathbf{K}}, i\omega_n) = \bar{G}(\vec{\mathbf{K}}, i\omega_n)^{-1} - \bar{G}(\vec{\mathbf{K}}, i\omega_n)^{-1}$. 8) Repeat from step 2) to step 7) until $\Sigma_c(\vec{\mathbf{K}}, i\omega_n)$ converges to desired accuracy. 9) Once convergence is reached, we can calculate the state density $\rho(\omega)$ by maximum entropy method [38]. And we can get other lattice quantities by some other additional analysis code.

By combining the DCA which introduces the nonlocal correlations and the exact numerical method: CTQMC, we can investigate the frustrated system efficiently. And it can be easily reconstructed to study another strong

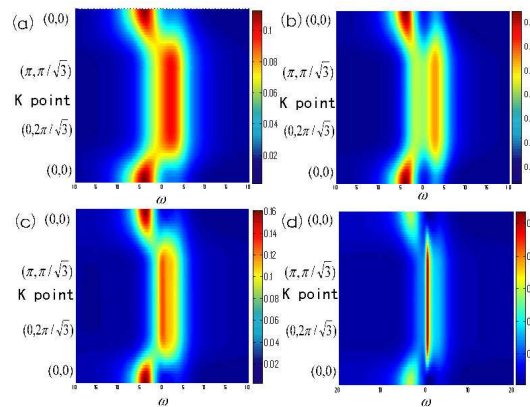


FIG. 5: (Color online) The K-dependent spectral function $A_k(\omega)$ for different temperature, when $a_s = 57a_0$. (a) At $T = 7.95nK$, the red part shows a Fermi-liquid-like peak near the Fermi energy. (b) At $T = 5.30nK$, a narrow pseudogap shown by the green region near $\omega = 0$. Two peak found around the pseudogap is shown by yellow and orange color. (c) At $T = 2.39nK$, a Fermi-liquid-like peak appears again shown by red color. (d) At $T = 0.95nK$, an obvious Kondo peak appears shown by red color near $\omega = 0$ line.

correlated system in the future research.

Phase Diagram. — We investigate the double occupancy $D_{occ} = \partial F / \partial U = \frac{1}{4} \sum_i \langle n_{i\uparrow} n_{i\downarrow} \rangle$ as a function of interaction U for various temperature, where F is the free energy. The D_{occ} is affected by the competition between the temperature and the interaction. When the interaction is lower than $70a_0$, the D_{occ} increases as the temperature decreases due to the enhancing of the itinerancy of atoms, as shown in Fig. 3, where the lattice depth V_0 is chosen to be $10E_T$. When the interaction is stronger than $70a_0$, the effect of the temperature on D_{occ} is weakened. The D_{occ} decreases as the interaction increases due to the suppressing of the itinerancy of the atoms. When the interaction is stronger than the critical interaction of the Mott transition, D_{occ} for different temperature is coincident, which shows the temperature does not affect the double occupancy distinctly. The continuity of the evolution of the double occupancy by interaction show that it is a second order transition.

We employ the maximum entropy method [38] to calculate the density of states (DOS) which describes the number of states at frequency ω . Fig. 4(a) shows DOS for different interaction at $T = 2.385nK$. There is a Fermi-liquid-like peak near the Fermi energy when $a_s = 32a_0$. A pseudogap formed by the splitting of Fermi-liquid-like peak appears when the interaction increases, such as $a_s = 65a_0$ and $a_s = 73a_0$. When the interaction is stronger than the critical interaction $a_s^c = 94a_0$, such as $a_s = 97a_0$ and $a_s = 162a_0$, the system becomes an insulator indicated by an opened gap. DOS for different interaction at $T = 1.193nK$ is shown in Fig. 4(b). When $a_s = 32a_0$, there is also a Fermi-liquid-like peak. When

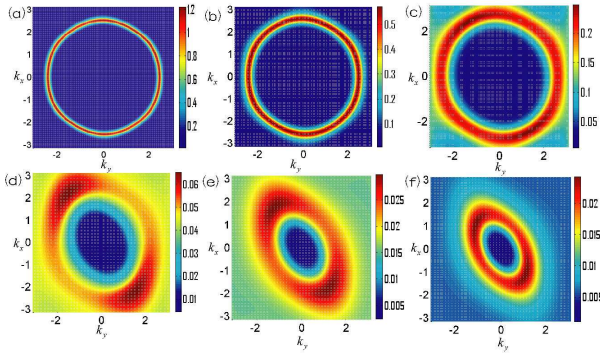


FIG. 6: (Color online) The Fermi surface as a function of momentum k for different interaction at $T = 0.68nK$: (a) $a_s = 53a_0$, (b) $a_s = 61a_0$, (c) $a_s = 67a_0$, (d) $a_s = 74a_0$, (e) $a_s = 81a_0$, (f) $a_s = 97a_0$.

the interaction increases, a Kondo resonance peak appears such as $a_s = 65a_0$, which is shown by a sharp quasi-particle peak with two shoulders. When $a_s = 75a_0$, the Kondo resonance peak is suppressed and a pseudogap appears, which is the intermediary state between the Fermi liquid and the Mott insulator. Similar with $T = 2.38nK$, a gap is opened after the interaction is stronger than the critical interaction $a_s^c = 86a_0$. Fig. 4(a) and (b) both show the evolution of the quasi-particle peak driven by the interaction is a continuity process, which means the transition is a second-order transition. Instead of directly splitting into two parts shown in Fig. 4(a), a Kondo peak appears, which is formed by the effect between the local atom and the itinerant atom at low temperature, as shown in Fig. 4(b).

We could also get the K-dependent spectral function $A_k(\omega) = -ImG_k(\omega + i0)/\pi$, which describes the distribution probability of the quasi-particle with momentum k and energy ω . Fig. 5 shows $A_k(\omega)$ for different temperature, where $a_s = 57a_0$. At $T = 7.95nK$, there exists a quasi-particle peak near the Fermi energy which shows a metallic behavior, as shown in Fig. 5(a). In Fig. 5(b), a pseudogap appears at $T = 5.3nK$, which is formed by the splitting of the quasi-particle peak. When $T = 2.39nK$, the pseudogap disappears and there is a quasi-particle peak again, as shown in Fig. 5(c). An obvious Kondo peak appears when $T = 0.95nK$, as shown in Fig. 5(d). It shows a reentrant behavior in the transition between Fermi liquid and pseudogap when the interaction is fixed and the temperature decreases. This behavior is based on the Kondo effect which suppresses the splitting of the quasi-particle peak at low temperature.

We study the Fermi surface as a function of momentum k by analyzing the maxima of the spectral weight at zero frequency: $A(k; \omega = 0) \approx -\frac{1}{\pi} \lim_{\omega_n \rightarrow 0} ImG(k, i\omega_n)$. A linear extrapolation of the first two Matsubara frequencies is used to estimate the self-energy to zero frequency [39]. Fig. 6 shows the Fermi surface for different inter-

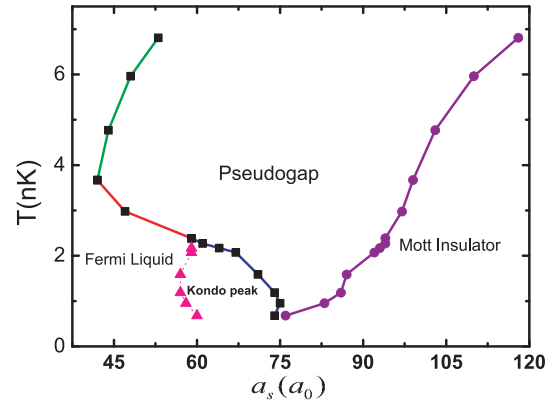


FIG. 7: (Color online) The phase diagram of Fermi atoms in triangular optical lattice, where the square plots with solid line (green, red, blue) indicate the transition line of the Fermi liquid and the pseudogap, the circular plots with solid line (purple) indicate the Mott transition line, the triangular plots with dash line (pink) mark the Kondo peak appearing region.

action at $T = 0.68nK$. A narrow ring which means the particles distribute on a certain energy displaying a behavior of metal, as shown in Fig. 6(a) and (b). As the interaction increases, the ring becomes bigger and the edge of the ring shows a hexangular shape, as shown in Fig. 6(c). This means the particles begin to be localized. In Fig. 6(d), the Fermi surface becomes an ellipse and the particles begin to distribute at the diagonal region. When the interaction is stronger than the critical interaction $a_s^c = 76a_0$, the Fermi surface does not change a lot, as shown in Fig. 6(e) and (f). Comparing with previous figures, the Fermi surface becomes a nearly flat plane. From Fig. 6(a) to Fig. 6(f), the amplitude of the spectral weight becomes small and the breadth become wider. The Fermi surface translates from a determined surface into a flat plane due to the localization of the particles when the interaction increases.

The phase diagram of cold atoms trapped in triangular optical lattice is shown in Fig. 7, where a_s indicates the s-wave scattering length. In the diagram, the translation between the Fermi liquid and the pseudogap shows a reentrant behavior. For a fixed interaction weaker than $58a_0$, when the temperature decreases, the system translates from Fermi liquid to pseudogap. When the temperature is lower than the critical temperature distributing on the red solid line, the system translates from pseudogap to Fermi liquid. There is a Kondo peak region, which is signed by the blue solid line and the pink dash line. If temperature is lower than $2.4nK$, a Kondo peak emerges before the appearing of the pseudogap when the interaction increases. However, if the temperature is higher than $2.4nK$ the system translates from Fermi Liquid to pseudogap directly. When the interaction is stronger than the critical interaction of Mott transition distributing on the purple line, the system translates from pseudogap to

insulator confirmed by an opened gap.

Experimental Protocol. — We design an experiment to investigate the quantum phase transition in triangular optical lattice. The experiment protocol can be taken as follows: The ^{40}K atoms can be firstly produced to be a pure fermion condensate by evaporative cooling [40, 41]. Then, three laser beams at wavelength $\lambda = 1064$ nm are used to form the triangular optical lattice to trap ^{40}K atoms. The lattice depth V_0 is used to adjust the kinetic energy t and the interaction U , such as $V_0 = 10E_r$. The on-site interaction can be adjusted by Feshbach resonance [42]. The s-wave scattering length is used to determine the effective interaction of cold atoms. When the interaction increases, the system translates from Fermi liquid ($a_s = 49a_0$) to Mott insulator ($a_s = 162a_0$) at temperature $T = 6.81\text{nK}$, as shown in Fig. 7. One spin component of the atoms on the double occupied sites can be transferred to a unpopulated magnetic sublevel by using a radio-frequency pulse. Then, the double occupancy D_{occ} can be deduced by the fraction of transformed atoms which is obtained by the absorption imaging technology [15]. At $T = 6.81\text{nK}$, D_{occ} decreases from 0.107 ($a_s = 49a_0$) to 0.00452 ($a_s = 162a_0$) with increasing atomic interaction. After switching off the confine potential, the atoms are allowed to take a ballistic expansion at the time scale of millisecond. Then, the Fermi surface can be obtained by taking an absorption imaging [40]. At $T = 6.81\text{nK}$, the circular ring shape of the Fermi surface when $a_s = 49a_0$ transforms into a flat elliptical ring when $a_s = 162a_0$.

Conclusion. — In conclusion, we propose an artificial system – cold atoms in triangular optical lattice, which is set up by three laser beams, to investigate the strong correlated effect in many body physics. The advantage of this artificial frustrated system is controllable and cleanliness. We show how the system evolves from Fermi liquid into Mott insulator for increasing interaction, and a reentrant behavior of the transition between Fermi liquid and pseudogap due to the Kondo effect at low temperature. Our study presents a helpful step for understanding the strong correlated effect in the frustrated system, such as the spin liquid. Beyond DMFT, DCA is improved to incorporate the nonlocal correlation which can not be simply ignored in the frustrated system. This numerical method is universally to investigate strongly correlated system, such as the high-temperature superconduc-

tor and the colossal magnetoresistance.

This work was supported by NSFC under grants Nos. 10874235, 10934010, 60978019, the NKBRFC under grants Nos. 2006CB921400, 2009CB930701 and 2010CB922904.

-
- [1] D. Jaksch et al., Phys. Rev. Lett. **81**, 3108 (1998).
 - [2] P. B. Blakie et al., J. Phys. B **37**, 1391 (2004).
 - [3] K. I. Petsas et al., Phys. Rev. A **50**, 5173 (1994).
 - [4] W. Hofstetter et al., Phys. Rev. Lett. **89**, 220407 (2002).
 - [5] Y. Inada et al., Phys. Rev. Lett. **101** 101, 180406 (2008).
 - [6] I. Bloch, Nature Physics **1**, 23 (2005).
 - [7] I. Bloch et al., Rev. Mod. Phys. **80**, 885 (2008).
 - [8] D. Jaksch, P. Zoller, Ann. Phys. (N. Y.) **315**, 52 (2005).
 - [9] L. M. Duan et al., Phys. Rev. Lett. **91**, 090402 (2003).
 - [10] L. Santos et al., Phys. Rev. Lett. **93**, 030601 (2004).
 - [11] B. Damski et al., Phys. Rev. A **72**, 053612 (2005).
 - [12] J. Ruostekoski, Phys. Rev. Lett. **103**, 080406 (2009).
 - [13] M. Greiner et al., Nature (London) **415**, 39 (2002).
 - [14] Y. Shin et al., Nature (London) **451**, 689 (2008).
 - [15] R. Jördans et al., Nature (London) **455**, 204 (2008).
 - [16] N. Gemelke et al., Nature (London) **460**, 995 (2009).
 - [17] U. Schneider et al., Science **322**, 1520 (2009).
 - [18] K. Aryanpour et al., Phys. Rev. B **74**, 085117 (2006).
 - [19] T. Ohashi et al., Phys. Rev. Lett. **100**, 076402 (2008).
 - [20] T. Yoshioka et al., Phys. Rev. Lett. **103**, 036401 (2009).
 - [21] D. Galanakis et al., Phys. Rev. B **79**, 115116 (2009).
 - [22] A. Liesch et al., Phys. Rev. B **79**, 195108 (2009).
 - [23] Z. W. Xie et al., Phys. Rev. A **70**, 045602 (2004).
 - [24] S. G. Bhongale et al., Phys. Rev. A **78**, 061606 (2008).
 - [25] P. B. He et al., Phys. Rev. A **76**, 043618 (2007).
 - [26] V. V. Konotop et al., Phys. Rev. A **65**, 021602 (2002).
 - [27] T. Ohashi et al., Phys. Rev. Lett. **97**, 066401 (2006).
 - [28] A. Georges et al., Rev. Mod. Phys. **68**, 13 (1996).
 - [29] W. Metzner et al., Phys. Rev. Lett. **62**, 324 (1989).
 - [30] E. Müller-Hartman, Z. Phys. B **76**, 211 (1989).
 - [31] R. W. Helmes et al., Phys. Rev. Lett. **100**, 056403 (2008).
 - [32] T. Maier et al., Rev. Mod. Phys. **77**, 1027 (2005).
 - [33] M. Jarrell et al., Phys. Rev. B **63**, 125102 (2001).
 - [34] M. Jarrell et al., Phys. Rev. B **64**, 195130 (2001).
 - [35] Y. Imai et al., Phys. Rev. B **65**, 233103 (2002).
 - [36] H. Lee et al., Phys. Rev. B **78**, 205117 (2008).
 - [37] A. N. Rubtsov et al., Phys. Rev. B **72**, 035122 (2005).
 - [38] M. Jarrell et al., Phys. Rep. **269**, 133 (1996).
 - [39] O. Parcollet et al., Phys. Rev. Lett. **92**, 226402 (2004).
 - [40] M. Köhl et al., Phys. Rev. Lett. **94**, 080403 (2005).
 - [41] J. K. Chin et al., Nature (London) **443**, 961 (2006).
 - [42] L. M. Duan, Phys. Rev. Lett. **95**, 243202 (2005).